Biophysical Journal
Article

Biophysical Society

Role of the Disulfide Bond in Prion Protein Amyloid Formation: A Thermodynamic and Kinetic Analysis

Ryo Honda[1,2,*]
[1]The United Graduate School of Drug Discovery and Medical Information Sciences and [2]Department of Molecular Pathobiochemistry, Graduate School of Medicine, Gifu University, Gifu, Japan

ABSTRACT Prion diseases are associated with the structural conversion of prion protein (PrP) to a β-sheet-rich aggregate, PrP^{Sc}. Previous studies have indicated that a reduction of the disulfide bond linking C179 and C214 of PrP yields an amyloidlike β-rich aggregate in vitro. To gain mechanistic insights into the reduction-induced aggregation, here I characterized how disulfide bond reduction modulates the protein folding/misfolding landscape of PrP, by examining 1) the equilibrium stabilities of the native (N) and aggregated states relative to the unfolded (U) state, 2) the transition barrier separating the U and aggregated states, and 3) the final structure of amyloidlike misfolded aggregates. Kinetic and thermodynamic experiments revealed that disulfide bond reduction decreases the equilibrium stabilities of both the N and aggregated states by ~3 kcal/mol, without changing either the amyloidlike aggregate structure, at least at the secondary structural level, or the transition barrier of aggregation. Therefore, disulfide bond reduction modulates the protein folding/misfolding landscape by entropically stabilizing disordered states, including the U and transition state of aggregation. This also indicates that the equilibrium stability of the N state, but not the transition barrier of aggregation, is the dominant factor determining the reduction-induced aggregation of PrP.

INTRODUCTION

Prion diseases have been associated with the structural conversion of cellular prion proteins (PrP) to an amyloidlike β-rich aggregate, PrP^{Sc} (1). PrP contains two cysteine residues at the positions of 179 and 214 (Fig. 1 *A*) (2). Previous in vitro studies have shown that the redox state of the disulfide bond linking the two cysteine residues is crucial for determining the amyloidogenic propensity of PrP (3–10). Although it remains elusive whether the in vivo conversion of PrP to PrP^{Sc} requires the breakage or shuffling of the disulfide bond (11–14), a reduction of the disulfide bond has been shown to decrease the thermal stability of PrP and trigger the formation of amyloidlike β-rich aggregates in vitro (3–10). In addition, the redox state of disulfide bonds has been closely associated with amyloid formation in various other systems, including insulin (15–18), tau (19,20), lysozyme (21,22), and β_2-microglobulin (23) (reviewed by Li et al. (24)). Therefore, it is important to elucidate how the redox state of the disulfide bond is linked to PrP aggregation in vitro.

To understand the role of the disulfide bond in PrP aggregation, I first considered a protein folding/misfolding landscape involving native, unfolded, and amyloid states (Fig. 1 *B*), and then deduced potential thermodynamic and kinetic mechanisms by which disulfide bond reduction affects the overall rate of protein aggregation. Here, at least three mechanisms are possible: disulfide bond reduction can affect the reaction pathway of protein aggregation to create an alternative pathway with a low free-energy barrier (mechanism I), decrease the equilibrium stability of the native state (ΔG_{N-U}) (mechanism II), or decrease the height of the kinetic barrier separating the monomeric and amyloid states of the protein ($\Delta G_{\ddagger-U}$) (mechanism III) (as further detailed in the Results and Discussion).

Although a general link between disulfide bond reduction and protein aggregation has been well described in a variety of systems (24), very few studies have investigated the underlying thermodynamic and kinetic mechanisms. Typically, in the case of globular proteins such as PrP, disulfide bond reduction is regarded as accelerating protein aggregation by decreasing ΔG_{N-U} (i.e., mechanism II) without full consideration of the folding/misfolding landscape. However, because each of three separate mechanisms could potentially contribute to the overall rate of protein aggregation (Fig. 1 *B*), no firm conclusion can be drawn without

Submitted October 10, 2017, and accepted for publication December 27, 2017.

*Correspondence: ryohonda.rh@gmail.com

Editor: James Shorter.
https://doi.org/10.1016/j.bpj.2017.12.031

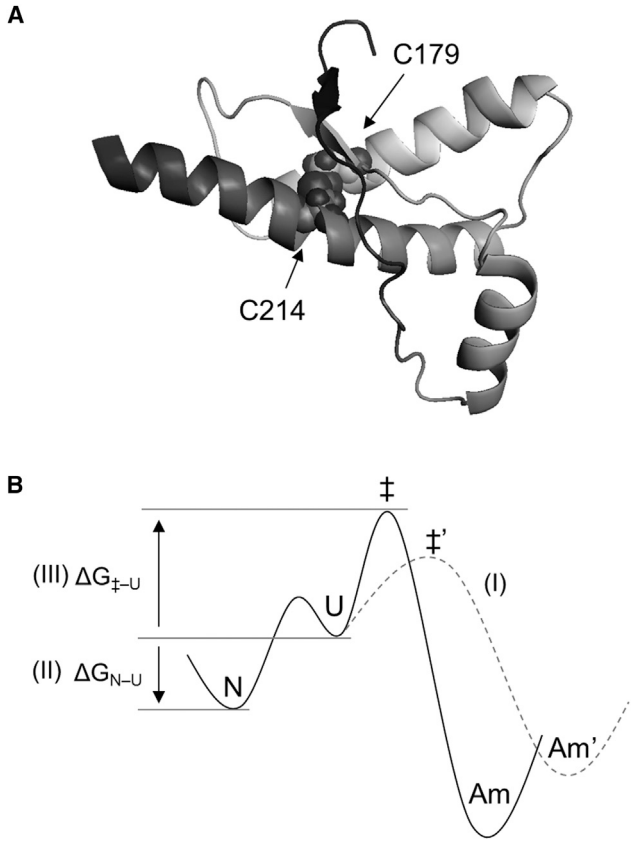

FIGURE 1 (*A*) NMR structure of the C-terminal domain of human PrP (residues 125–228) (PDB: 1QLZ). The disulfide bond connecting C179 and C214 is highlighted as spheres. (*B*) The aggregation pathway from the native state (N) to an aggregated state (Am) via an amyloidogenic unfolded state (U), together with three possible mechanisms affecting the overall rate of protein aggregation: (I) change in the reaction pathway, (II) change in the free-energy difference between the N and U states (ΔG_{N-U}), and (III) change in the free-energy difference between the U and transition (‡) states ($\Delta G_{‡-U}$).

comprehensive understanding of the folding/misfolding landscape. Therefore, in this study, I initially examined how disulfide bond reduction modulates the folding/misfolding landscape of PrP by testing the above-described three mechanisms, and then discussed which mechanism is primarily responsible for the reduction-induced aggregation of PrP.

MATERIALS AND METHODS

Amyloid formation

Amyloid fibrils were prepared from recombinant C-terminal fragments of human PrP (residues 124–230) according to a protocol to be published elsewhere. Briefly, a 250-μM protein solution containing 6 M guanidine hydrochloride (GuHCl) and 10 mM Tris-HCl (pH 8) was initially incubated for 1 h at 37°C in the presence or absence of 5 mM (5 mM Tris(2-carboxyethyl)phosphine, TCEP) to cleave the disulfide bond and remove any preexisting aggregates. This solution was subsequently diluted to a final concentration of 25 μM in 25 mM HEPES buffer (pH 7.4) containing 0.02% NaN_3, and 2 or 3 M GuHCl, with or without 5 mM TCEP. The reaction mixture was rotated at 1000 RPM and 37°C, and amyloid fibril assembly were monitored by change in ThT fluorescence at 485 nm (excitation wavelength of 445 nm) in aliquots of the reaction mixtures collected at various time points. The time courses of ThT fluorescence were fitted to a sigmoidal equation to estimate the lag time (t_{lag}) of amyloid formation:

$$F(t) = \frac{\text{maximum}}{1+\exp\left(\frac{t_{half}-t}{\text{rate}}\right)},$$

$$t_{lag} = t_{half} - 2 \times (\text{rate}) \times (\text{maximum}).$$

Solubility and stability studies for monomeric PrP

A 250-μM solution of protein was initially incubated under the reducing condition as described above, diluted to a final concentration of 10 or 25 μM in 5 mM HEPES buffer (pH 7.4) containing various concentrations of GuHCl with or without 1 mM TCEP, and incubated for 1 h at 37°C. The reaction mixture was then centrifuged at 62,900 $\times$ *g* for 30 min to remove insoluble aggregates, and the protein concentration in the soluble fraction (i.e., supernatant) was determined by the UV absorbance analysis (ε_{280} = 16,640 $cm^{-1}M^{-1}$). Soluble proteins with concentrations $\geq$1 μM in the supernatant were subsequently subjected to far-UV CD according to a previously published protocol (25).

Ellman reaction

To determine the redox states of amyloid fibrils, 200 μL of the amyloid solution was centrifuged at 62,900 $\times$ *g* for 30 min, and the resulting pellet was washed twice with cooled acidic buffer (pH 4, 20 mM sodium acetate) to remove residual reducing agents. The pellet was then resuspended with 100 μL of a denaturing buffer (pH 4, 20 mM sodium acetate and 6 M guanidine thiocyanate) and incubated at 37°C for 30 min to dissociate the amyloid fibrils into consecutive monomers. Undissociated amyloid fibrils were removed by centrifugation at 62,900 $\times$ *g* for 30 min at 37°C. The protein concentration of a 90 μL aliquot of the resulting supernatant supplemented with 10 μL of 1 M Tris-HCl buffer (pH 8) was determined by UV absorbance at 280 nm. The protein concentration in the supernatant (29.0 $\pm$ 2.6 and 45.9 $\pm$ 7.1 μM for oxidized and reduced proteins, respectively) suggested that 58 and 91% of the total input were recovered from oxidized and reduced amyloid fibrils, respectively. The protein solution was immediately supplemented with 1 μL of 20 mg/mL 5,5′-dithiobis(2-nitrobenzoic acid) (DTNB) in DMSO (equivalent to 50 mM), and incubated at room temperature and in the dark for 3 min. Finally, the absorbance at 412 nm was measured to determine the free –SH concentration using the Ellman method (ε = 13,700 $M^{-1}cm^{-1}$) (26). The number of free –SH groups per protein molecule was determined by dividing the free –SH concentration by the protein concentration. DTNB was purchased from Nacalai Tesque (Cat. No. 14101-21; Kyoto, Japan) and dissolved with DMSO just before use.

Structural analyses of amyloid fibrils

TEM, Fourier-transform infrared (FTIR), and proteinase-K digestion were performed using standard procedures for which the details will be published elsewhere.

GuHCl-unfolding experiment

The GuHCl-unfolding curve for oxidized PrP monomer was fitted to a two-state unfolding model:

$$\Theta[\mathrm{GuHCl}] = n_i \times \frac{1}{1+K} + (u_i + u_s[\mathrm{GuHCl}]) \times \frac{K}{1+K},$$

$$K = \exp\left(\frac{\Delta G_{N-U} - m \times [\mathrm{GuHCl}]}{\mathrm{RT}}\right).$$

The best fit values were as follows: −3.09 kcal/mol for ΔG, −1.68 kcal/mol M for m, −14162 degrees^{-1} cm^2 dmol^{-1} for n_i, −2945 degrees^{-1} cm^2 dmol^{-1} for u_i, and 282 degrees^{-1} cm^2 dmol^{-1}/M for u_s.

For the analysis of amyloid fibrils, a solution containing amyloid fibrils (25 μM in monomer equivalent units) was diluted 10-fold in a buffer containing 5 mM HEPES (pH 7.4), various concentrations of GuHCl (0–8.7 M) and 0 or 1 mM TCEP. The resulting solution was incubated at 37°C for 24 h and subsequently diluted fivefold with a ThT buffer [pH 8, 62.5 mM Tris-HCl, 6.25 μM ThT, and various concentration of GuHCl (0–2.0 M)] to adjust the final GuHCl concentration to 1.6 M. This dilution step is of importance, because ThT fluorescence strongly depends on the GuHCl concentration (27). Within 1 min after dilution, ThT fluorescence of the solution was measured using the above-described procedure. The GuHCl-unfolding curves were analyzed using a linear polymerization model proposed by Narimoto et al. (28):

$$F[\mathrm{GuHCl}] = s \times \sum_{i=1}^{\infty} i[P_i] = s \times \left([\mathrm{M}]_0 - [\mathrm{M}]\right)$$

$$= s \times \left([\mathrm{M}]_0 - \frac{2[\mathrm{M}]_0 K_a + 1 - \sqrt{4[\mathrm{M}]_0 K_a + 1}}{2[\mathrm{M}]_0 K_a^2}\right),$$

$$K_a = \exp\left(\frac{\Delta G_{\mathrm{Am-U}} - m \times [\mathrm{GuHCl}]}{\mathrm{RT}}\right),$$

where s represents the ThT-fluorescence per mass concentration of amyloid fibrils. The best fit values [ΔG (kcal/mol), m (kcal/mol M), and s (a.u./μM)] were as follows: −5.95, −1.14, and 0.28 for oxidized amyloid fibrils, −2.90, −0.98, and 0.32 for reduced amyloid fibrils. $[\mathrm{M}]_0$ was fixed to 2.5 μM.

RESULTS AND DISCUSSION

Reducing the disulfide bond of PrP

The C-terminal domain of human PrP with an intact disulfide bond was expressed and purified according to a previously published protocol (25). The presence of the disulfide bond was previously confirmed using analytical reverse-phase HPLC and solution NMR (data not shown). To examine the role of this disulfide bond in amyloid formation, the protein was initially reduced by 1-h incubation at 37°C in the presence of a reducing agent (TCEP) and denaturant (GuHCl) at pH 8. Consistent with previous studies (5,6), the reduced PrP exhibited a high propensity to form amorphous aggregates when diluted in a denaturant-free buffer at pH 7.4. Under these conditions, no PrP was detected in the soluble fraction after centrifugation at 62,900 × g for 30 min (Fig. 2 *A*).

Many studies of amyloid formation have used moderate concentrations of GuHCl to facilitate this reaction by destabilizing the native structure of oxidized PrP (25,29–33). As amorphous aggregate formation observed in reduced PrP might compete with amyloid formation (34), I similarly applied a moderate concentration of GuHCl to dissolve these undesirable amorphous aggregates into soluble monomers (Fig. 2 *A*). Reduced PrP gradually appeared in the soluble fraction, with increasing concentrations of GuHCl from 0 to 1.5 M, and, above 2 M, the protein was fully recovered in the soluble fraction. I therefore used GuHCl at concentrations exceeding 2 M in the following evaluations of amyloid formation kinetics.

Disulfide bond reduction accelerates amyloid formation at 2 M GuHCl

I initially sought to examine the effect of disulfide bond reduction on amyloid formation at 2 M GuHCl. To this

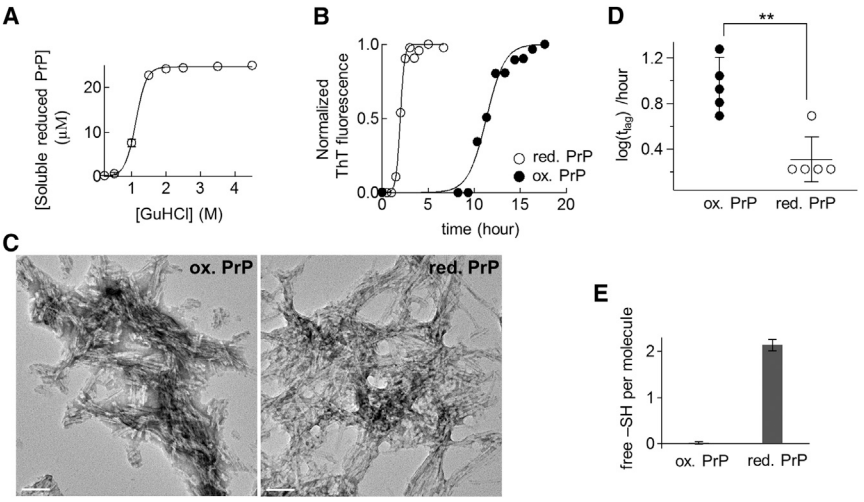

FIGURE 2 (*A*) Solubilities of PrP at various concentrations of GuHCl. Reduced PrP (25 μM) was incubated for 1 h at 37°C in the presence of various concentrations of GuHCl and centrifuged at 62,900 × g for 30 min. The concentration of soluble protein was measured using UV absorbance at 280 nm. (*B*) Representative time courses of amyloid formation from oxidized (*solid circles*) and reduced PrP (*open circles*) at a GuHCl concentration of 2 M. ThT-fluorescence was normalized to its maximum value (346 ± 96 and 740 ± 380 a.u. for oxidized and reduced proteins, respectively). The solid lines represent best fits to a sigmoidal function. (*C*) Transmission electron micrographs of the amyloid fibrils generated from oxidized (left) or reduced PrP (*right*). Scale bars, 100 nm. (*D*) Lag time of amyloid formation derived from Fig. 2 *B* (**$p < 0.005$, unpaired two-tailed t-test). (*E*) The number of free –SH group detected in a protein monomer dissociated from amyloid fibrils.

end, a reaction mixture containing either oxidized or reduced soluble PrP was agitated to initiate rapid amyloid formation, and the progress of the reaction was monitored by changes in the thioflavin T (ThT) fluorescence. As shown in Fig. 2 *B*, both forms of protein exhibited increases in ThT fluorescence after 4–10 h of lag phase, consistent with the typical formation kinetics of amyloid fibrils. Transmission electron micrographs of the final reaction products (Fig. 2 *C*) demonstrated that both oxidized and reduced samples exhibited the typical morphological characteristics of amyloid fibrils, where linear fibrillar aggregates were predominantly observed. Clearly, these results demonstrate that both the oxidized and reduced forms of PrP can yield morphologically similar amyloid fibrils. However, a comparison of the two sigmoidal curves (Fig. 2 *B*) indicates that reduced PrP has a shorter lag time (t_{lag}) for amyloid formation relative to oxidized PrP (Fig. 2 *D*), suggesting that disulfide bond reduction accelerates amyloid formation at 2 M GuHCl.

To determine whether or not the disulfide bond is present in the final structure of amyloid fibrils, I next examined the redox states of amyloid fibrils using a thiol-reactive agent, DTNB, according to the Ellman method (26). Here, the amyloid fibrils formed from oxidized or reduced PrP were initially separated from residual monomers by centrifugation at 62,900 × *g* for 30 min, and subsequently dissociated into constitutive monomers under acidic conditions (6 M guanidine thiocyanate, pH 4). Next, the standard Ellman assay was used to quantify the number of free thiol groups in the individual protein monomers (for more details, see Materials and Methods). As shown in Fig. 2 *E*, the protein monomer dissociated from reduced amyloid fibrils contained two free thiol groups per molecule, consistent with the number of the cysteine residues in the amino acid sequence of PrP. By contrast, no free thiol groups were detected in the protein monomers dissociated from oxidized amyloid fibrils, indicating that all cysteine residues had formed the intramolecular disulfide bond. These results confirm that the redox states of PrP remained unchanged during structural conversion from monomers to amyloid fibrils in this experiment.

Three potential mechanisms affecting the rate of amyloid formation

At least three mechanisms may underlie the high amyloidogenic propensity of reduced PrP. Fig. 1 *B* illustrates a simplified amyloid formation pathway from the native state (N) to amyloid fibrils (Am) via an amyloidogenic unfolded state (U), together with three possible mechanisms affecting the overall rate of amyloid formation. The first mechanism assumes that disulfide bond reduction alters the reaction pathway of amyloid formation such that the height of the kinetic barrier is decreased ($\Delta G_{N-\ddagger'} < \Delta G_{N-\ddagger}$, mechanism I). This mechanism can be experimentally tested by comparing the final structures of amyloid fibrils and determining whether the final state of oxidized and reduced proteins is identical (Am) or not (Am′). Strictly speaking, however, a change in the reaction pathway does not always lead to a detectable change in the final structure of amyloid fibrils. Therefore, it is virtually impossible to completely rule out or confirm mechanism I through a structural comparison. The second and third mechanisms respectively assume that disulfide bond reduction affects the free-energy differences between the N and U states (ΔG_{N-U}, mechanism II) and between the U and transition states ($\Delta G_{\ddagger-U}$, mechanism III). As the total height of the kinetics barrier of amyloid formation ($\Delta G_{N-\ddagger}$) is represented by the sum of ΔG_{N-U} and $\Delta G_{U-\ddagger}$, these two values are particularly important with respect to the overall rate of protein aggregation. Mechanisms II and III can be easily tested using simple thermodynamic and kinetic experiments, as described below. In the following sections, I will examine which mechanism contributes predominantly to the strong amyloidogenic propensity of reduced PrP.

Structural effects of disulfide bond reduction on amyloid fibrils

To address whether disulfide bond reduction affects the reaction pathway of amyloid formation (mechanism I), I examined amyloid fibril structures using FTIR spectroscopy and the proteinase K (PK) digestion assay. These assays are widely used to detect structural differences (polymorphisms) of amyloidlike aggregates with good sensitivity (35–37). As shown in Fig. 3 *A*, the FTIR spectra and second derivatives of oxidized and reduced amyloid fibrils overlapped completely, indicating a common secondary structure content. The position of the peak bond (1621 cm^{-1}) indicated that both amyloid fibrils were enriched with the intermolecular β-sheet structure (38). Fig. 3 *B* shows the results of PK-digestion assay for both proteins. Although a marked increase in PK-resistance was observed for both proteins upon the conversion from monomers of amyloid fibrils, no clear difference in the PK digestion pattern was observed in the amyloid forms, indicating that both amyloid fibrils shared a common PK resistant core at the C-terminal residues (27,29,31,39,40). The observed slight difference in the band intensity (i.e., oxidized amyloid fibrils appeared to produce a more intense band relative to reduced amyloid fibrils) likely reflect a difference in equilibrium stability rather than in structure (see Fig. 4 *B*). Therefore, disulfide bond reduction does not affect the final structure of amyloid fibrils, at least at the secondary structural level, and the oxidized and reduced proteins seem to use the same reaction pathway for amyloid formation. However, a further study using high-resolution techniques is required to determine whether disulfide bond reduction affects the tertiary and quaternary structure of amyloid fibrils.

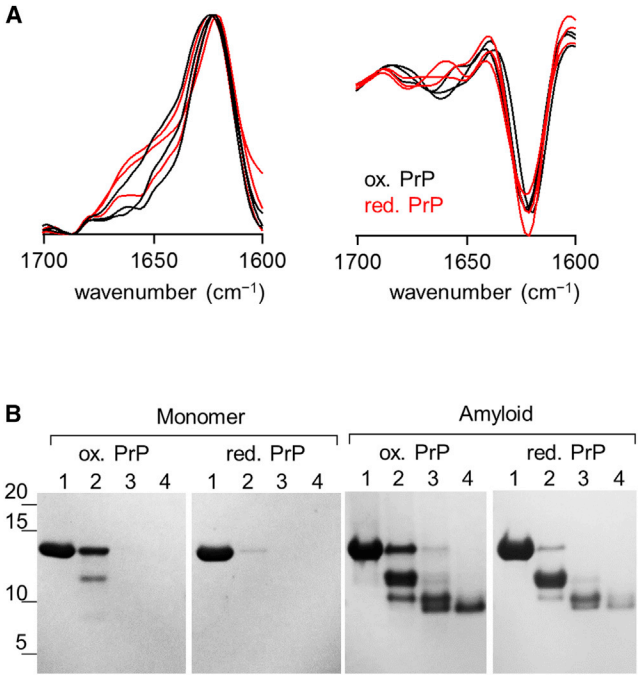

FIGURE 3 (*A*) FTIR spectra (*left*) and corresponding second derivatives (*right*) of oxidized (*black lines*) and reduced amyloid fibrils (*red lines*) were recorded using the attenuated total reflection in a D_2O buffer at pD 6.0. The FTIR spectra are normalized with respect to the peak intensity at 1621 cm^{-1}. Three spectra obtained from different preparations of amyloid fibrils are shown. (*B*) PK-resistant fragments of PrP monomers (*left*) and amyloid fibrils (*right*) were analyzed by tricine-SDS-PAGE and CBB staining. Here, protein monomers or amyloid fibrils (12.5 μM in the monomer equivalent units) were treated with 0 (lane 1), 0.0125 (lane 2), 0.125 (lane 3), or 1.25 μM PK (lane 4) at 37°C for 1 h at pH 7.4 in the presence of 1 M GuHCl. To see this figure in color, go online.

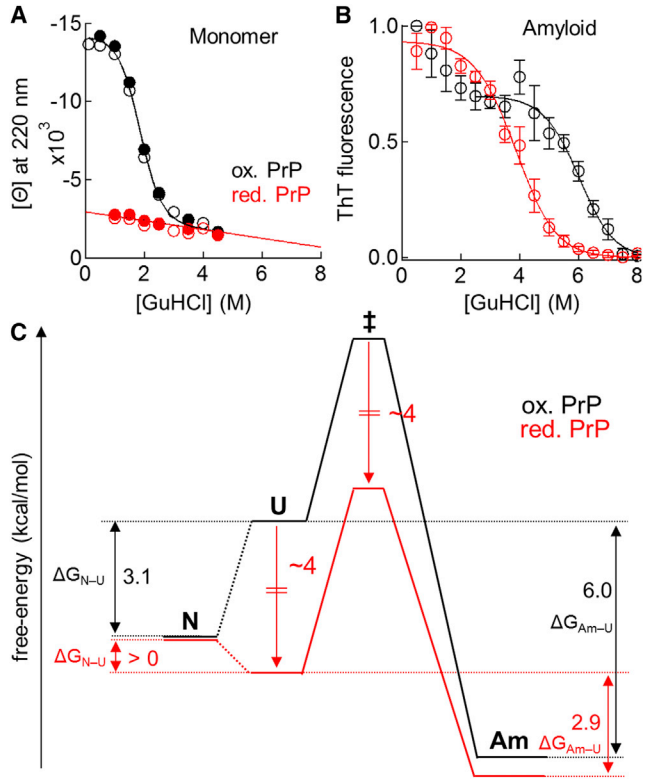

FIGURE 4 (*A*) GuHCl-unfolding curves for the monomeric forms of oxidized (*black circles*) and reduced PrP (*red circles*) at the protein concentration of 10 (*open circles*) or 25 μM (*solid circles*). (*B*) GuHCl-unfolding curves for amyloid fibrils generated from oxidized (*black open circles*) and reduced PrP (*red open circles*). Data represent mean values ± standard deviations from three experiments that used different preparations of amyloid fibrils. (*C*) Effects of disulfide bond reduction on the free-energy landscape of protein misfolding at a protein concentration of 2.5 μM in a denaturant-free solution. Disulfide bond reduction decreased the free-energies of the unfolded (U) and transition states (‡) by ~3–4 kcal/mol, without significantly changing the free-energies of the native state (N) and amyloid fibrils (Am), leading to net destabilization effects of >3.1 kcal/ mol on the N state (Fig. 4 *A*), 3.1 kcal/mol on the Am state (Fig. 4 *B*), but ~0 kcal/mol on the ‡ state when compared to the U state (Fig. 5 *B*). To see this figure in color, go online.

Effect on the equilibrium stability of the N state

Next, I performed GuHCl-unfolding experiments to examine whether disulfide bond reduction would affect the equilibrium stability of the N state (mechanism II). The GuHCl-unfolding curves for the monomeric forms of oxidized and reduced PrP were obtained using far-UV circular dichroism (Fig. 4 *A*). Curve-fitting using a two-state unfolding model indicated that the oxidized protein existed as a 4:6 mixture of the N and U states at 2 M GuHCl, whereas the reduced protein existed as the pure U state at the same concentration of GuHCl, suggesting that disulfide bond reduction decreased the proportion of the N state and simultaneously increased the proportion of the U state. A comparison of the two GuHCl-unfolding curves led to rough estimation that disulfide bond reduction destabilized the N state by a minimum of 3.1 kcal/mol in denaturant-free solution (a precise value was not obtained because reduced PrP precipitated as an amorphous aggregate at low concentrations of GuHCl) (Table 1). A similar destabilizing effect of disulfide bond reduction has been reported in previous publications examining PrP folding (3–6). Therefore, disulfide bond reduction decreases the equilibrium stability of the N state, suggesting that mechanism II at least partly contributes to the strong amyloidogenic propensity of reduced PrP at 2 M GuHCl.

Effect on the kinetic barrier of aggregation

To measure effect of the disulfide bond on the height of the free-energy barrier ($\Delta G_{‡–U}$), I repeated the above kinetic

TABLE 1 Equilibrium Stabilities of Monomers and Amyloid Fibrils in Oxidized and Reduced Forms

	ΔG_{ox}	ΔG_{red}	$\Delta\Delta G$ ($\Delta G_{red}-\Delta G_{ox}$)
Monomer ($\Delta G_{N–U}$)	−3.1 ± 0.1	<0	>3.1
Amyloid fibril ($\Delta G_{Am–U}$)	−6.0 ± 1.1	−2.9 ± 0.1	3.1 ± 1.1

Measured in kcal/mol.

experiment at a higher concentration of GuHCl (3 M), where both oxidized and reduced PrP existed in an almost pure U state (N state: <5%, Fig. 4 *A*). The rationale behind this experiment is that if a protein exists in a pure U state, then the rate of amyloid formation should reflect the $\Delta G_{U-\ddagger}$ without any contribution from ΔG_{N-U}. Previously, Dutta et al. (41) used this approach to demonstrate that S170N/N174T mutation enhanced the amyloidogenic propensity of PrP mainly by decreasing $\Delta G_{\ddagger-U}$, but not ΔG_{N-U}. Here, I chose the minimum GuHCl concentration required for PrP unfolding because, at higher GuHCl concentrations (>4 M), the reverse reaction (i.e., the dissociation of amyloid fibrils) becomes nonnegligible and thus complicates the kinetics of amyloid formation.

Remarkably, as shown in Fig. 5, *A* and *B*, the oxidized and reduced PrP did not differ significantly in terms of t_{lag} under the fully unfolded conditions (3 M GuHCl), indicating that disulfide bond reduction does not affect the rate of amyloid formation when the N state is completely disrupted. In other words, disulfide bond reduction does not affect the $\Delta G_{\ddagger-U}$, thus ruling out mechanism III. This result has an additional implication regarding the structure of the transition state (‡) during amyloid formation. Specifically, the finding that disulfide bond reduction stabilizes ‡ by the same extent as the U state indicates that the two segments containing residues C179 and C214 (i.e., H2 and H3) are not associated in ‡ (for more details, see Fig. 3 in (42)).

Destabilization of the N state drives reduction-induced aggregation

Taken together, the results of the above series of experiments indicate that disulfide bond reduction accelerates amyloid formation mainly by destabilizing the N state (mechanism II). By contrast, the reaction pathway of amyloid formation (mechanism I) and the height of the free-energy barrier separating the U state from the amyloid state (mechanism III) appear to remain unchanged upon disulfide bond reduction. These experiments led me to conclude that disulfide bond reduction enhances the amyloidogenic propensity of PrP mainly by destabilizing the N state.

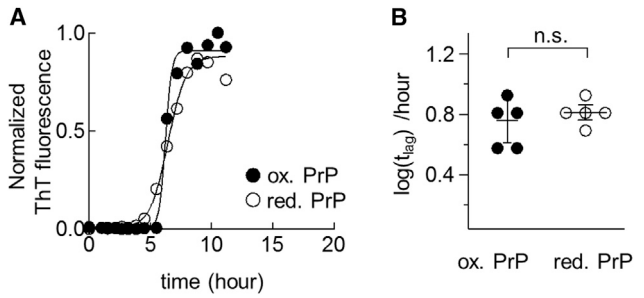

FIGURE 5 (*A*) Representative time courses of amyloid formation from oxidized (*solid circles*) and reduced PrP (*open circles*) at 3 M GuHCl. ThT-fluorescence was normalized to its maximum value (353 ± 61 and 481 ± 92 a.u. for oxidized and reduced proteins, respectively). The solid lines represent the best fits to a sigmoidal function. (*B*) Lag times of amyloid formation were derived from Fig. 5 *A* (n.s., $p > 0.05$, unpaired two-tailed *t*-test).

Effect on the equilibrium stability of amyloid fibrils

The equilibrium stability of amyloid fibrils relative to the U state (ΔG_{Am-U}) is an important parameter both for characterizing the overall folding/misfolding landscape as and for determining whether the disulfide bond is beneficial for the stability of amyloid fibrils. I therefore examined the effect of disulfide bond reduction on ΔG_{Am-U} using the GuHCl-unfolding assay. This assay has been widely used to estimate ΔG_{Am-U}, based on the linear-polymerization model of amyloid formation (28,43). Because the amyloid fibrils were insufficiently soluble to allow a far-UV CD measurement, in this study, the GuHCl-unfolding curves were determined by measuring ThT fluorescence.

As shown in Fig. 4 *B*, the reduced and oxidized amyloid fibrils represented the major unfolding transitions in 2–6 M GuHCl and 5–8 M GuHCl, respectively. The lower shift of the unfolding curve clearly indicates that disulfide bond reduction destabilizes the amyloid fibrils and thus increases ΔG_{Am-U}. Although the oxidized amyloid fibrils represented an additional transition at lower GuHCl concentrations (0–2 M) (Fig. 4 *B*), I ignored this transition in the subsequent analysis. This is because the oxidized PrP monomer exists as an equilibrium between the N and U states at low GuHCl concentrations (1–2.5 M, Fig. 4 *A*), and thus the GuHCl-unfolding of amyloid fibrils depends not only on ΔG_{Am-U} but also on ΔG_{N-U}. Such complexity can be reduced by ignoring the low GuHCl concentration data. Accordingly, by fitting the GuHCl-unfolding curves of oxidized (only 3–8 M) and reduced (0–8 M) amyloid fibrils to the linear polymerization model, ΔG_{Am-U} was estimated as -6.0 ± 1.1 and -2.9 ± 0.1 kcal/mol, respectively. Therefore, disulfide bond reduction destabilized amyloid fibrils, and increased ΔG_{Am-U} by 3.1 ± 1.1 kcal/mol (Table 1).

Interestingly, the destabilizing effect of the disulfide bond reduction on amyloid fibrils ($\Delta\Delta G_{Am-U} = 3.1 \pm 1.1$ kcal/mol) is very similar to the effect on the N state ($\Delta\Delta G_{N-U} > 3.1$ kcal/mol), indicating that the decrease in the stabilities of these two states is mainly conferred by an ~3–4 kcal/mol decrease in the free energy of the reference state (i.e., U state) (Fig. 4 *C*). Disulfide bond reduction typically increases the entropy of U state by removing conformational constraints imposed by the disulfide bond and leading to a substantial decrease in the free energy (42). The Pace equation estimated that the entropic effect contributes to ~4 kcal/mol decrease in the free energy of the U state (44), which is reasonably consistent with the $\Delta\Delta G_{Am-U}$ and $\Delta\Delta G_{N-U}$ values. This result indicates that, by decreasing the free energy of the U state without

changing the free energies of either the N state or amyloid fibrils, disulfide bond reduction leads to a net destabilization of the two latter states. This in turn implicates that the disulfide bond connecting C179 and C214 is accommodated in a very restricted manner in the N state and amyloid fibrils, such that disulfide bond reduction does not increase the entropy and free energies of these two states.

AUTHOR CONTRIBUTIONS

R.H. designed and performed all the experiments, analyzed the data, and wrote the manuscript.

ACKNOWLEDGMENTS

The author thanks Kazuo Kuwata for use of laboratory analytical instruments, and Enago (https://www.enago.jp) for the English language review.

This work was supported by JSPS KAKENHI grant No. 16J04145.

REFERENCES

1. Colby, D. W., and S. B. Prusiner. 2011. Prions. *Cold Spring Harb. Perspect. Biol.* 3:a006833.
2. Zahn, R., A. Liu, …, K. Wüthrich. 2000. NMR solution structure of the human prion protein. *Proc. Natl. Acad. Sci. USA.* 97:145–150.
3. Eberl, H., and R. Glockshuber. 2002. Folding and intrinsic stability of deletion variants of PrP(121–231), the folded C-terminal domain of the prion protein. *Biophys. Chem.* 96:293–303.
4. Mehlhorn, I., D. Groth, …, S. B. Prusiner. 1996. High-level expression and characterization of a purified 142-residue polypeptide of the prion protein. *Biochemistry.* 35:5528–5537.
5. Zhang, H., J. Stockel, …, F. E. Cohen. 1997. Physical studies of conformational plasticity in a recombinant prion protein. *Biochemistry.* 36:3543–3553.
6. Maiti, N. R., and W. K. Surewicz. 2001. The role of disulfide bridge in the folding and stability of the recombinant human prion protein. *J. Biol. Chem.* 276:2427–2431.
7. Jackson, G. S., L. L. Hosszu, …, J. Collinge. 1999. Reversible conversion of monomeric human prion protein between native and fibrillogenic conformations. *Science.* 283:1935–1937.
8. Hosszu, L. L., C. R. Trevitt, …, A. R. Clarke. 2009. Conformational properties of β-PrP. *J. Biol. Chem.* 284:21981–21990.
9. Trevitt, C. R., L. L. Hosszu, …, A. R. Clarke. 2014. N-terminal domain of prion protein directs its oligomeric association. *J. Biol. Chem.* 289:25497–25508.
10. Lee, S., and D. Eisenberg. 2003. Seeded conversion of recombinant prion protein to a disulfide-bonded oligomer by a reduction-oxidation process. *Nat. Struct. Biol.* 10:725–730.
11. Herrmann, L. M., and B. Caughey. 1998. The importance of the disulfide bond in prion protein conversion. *Neuroreport.* 9:2457–2461.
12. Welker, E., L. D. Raymond, …, B. Caughey. 2002. Intramolecular versus intermolecular disulfide bonds in prion proteins. *J. Biol. Chem.* 277:33477–33481.
13. Turk, E., D. B. Teplow, …, S. B. Prusiner. 1988. Purification and properties of the cellular and scrapie hamster prion proteins. *Eur. J. Biochem.* 176:21–30.
14. Stahl, N., M. A. Baldwin, …, S. B. Prusiner. 1993. Structural studies of the scrapie prion protein using mass spectrometry and amino acid sequencing. *Biochemistry.* 32:1991–2002.
15. Zako, T., M. Sakono, …, M. Maeda. 2009. Bovine insulin filaments induced by reducing disulfide bonds show a different morphology, secondary structure, and cell toxicity from intact insulin amyloid fibrils. *Biophys. J.* 96:3331–3340.
16. Devlin, G. L., T. P. Knowles, …, C. E. MacPhee. 2006. The component polypeptide chains of bovine insulin nucleate or inhibit aggregation of the parent protein in a conformation-dependent manner. *J. Mol. Biol.* 360:497–509.
17. Maeda, R., K. Ado, …, Y. Taniguchi. 2007. Promotion of insulin aggregation by protein disulfide isomerase. *Biochim. Biophys. Acta.* 1774:1619–1627.
18. Li, Y., H. Gong, …, K. Huang. 2012. Dissecting the role of disulfide bonds on the amyloid formation of insulin. *Biochem. Biophys. Res. Commun.* 423:373–378.
19. Stöhr, J., H. Wu, …, W. F. DeGrado. 2017. A 31-residue peptide induces aggregation of tau's microtubule-binding region in cells. *Nat. Chem.* 9:874–881.
20. Bhattacharya, K., K. B. Rank, …, S. K. Sharma. 2001. Role of cysteine-291 and cysteine-322 in the polymerization of human tau into Alzheimer-like filaments. *Biochem. Biophys. Res. Commun.* 285:20–26.
21. Cao, A., D. Hu, and L. Lai. 2004. Formation of amyloid fibrils from fully reduced hen egg white lysozyme. *Protein Sci.* 13:319–324.
22. Yang, M., C. Dutta, and A. Tiwari. 2015. Disulfide-bond scrambling promotes amorphous aggregates in lysozyme and bovine serum albumin. *J. Phys. Chem. B.* 119:3969–3981.
23. Ohhashi, Y., Y. Hagihara, …, Y. Goto. 2002. The intrachain disulfide bond of β(2)-microglobulin is not essential for the immunoglobulin fold at neutral pH, but is essential for amyloid fibril formation at acidic pH. *J. Biochem.* 131:45–52.
24. Li, Y., J. Yan, …, K. Huang. 2013. Disulfide bonds in amyloidogenesis diseases related proteins. *Proteins.* 81:1862–1873.
25. Honda, R. P., and K. Kuwata. 2017. The native state of prion protein (PrP) directly inhibits formation of PrP-amyloid fibrils in vitro. *Sci. Rep.* 7:562.
26. Winther, J. R., and C. Thorpe. 2014. Quantification of thiols and disulfides. *Biochim. Biophys. Acta.* 1840:838–846.
27. Bocharova, O. V., L. Breydo, …, I. V. Baskakov. 2005. Synthetic prions generated in vitro are similar to a newly identified subpopulation of PrPSc from sporadic Creutzfeldt-Jakob disease. *Protein Sci.* 14:1222–1232.
28. Narimoto, T., K. Sakurai, …, Y. Goto. 2004. Conformational stability of amyloid fibrils of β2-microglobulin probed by guanidine-hydrochloride-induced unfolding. *FEBS Lett.* 576:313–319.
29. Cobb, N. J., F. D. Sönnichsen, …, W. K. Surewicz. 2007. Molecular architecture of human prion protein amyloid: a parallel, in-register β-structure. *Proc. Natl. Acad. Sci. USA.* 104:18946–18951.
30. Bocharova, O. V., L. Breydo, …, I. V. Baskakov. 2005. In vitro conversion of full-length mammalian prion protein produces amyloid form with physical properties of PrP(Sc). *J. Mol. Biol.* 346:645–659.
31. Singh, J., and J. B. Udgaonkar. 2013. Dissection of conformational conversion events during prion amyloid fibril formation using hydrogen exchange and mass spectrometry. *J. Mol. Biol.* 425:3510–3521.
32. Milto, K., K. Michailova, and V. Smirnovas. 2014. Elongation of mouse prion protein amyloid-like fibrils: effect of temperature and denaturant concentration. *PLoS One.* 9:e94469.
33. Kocisko, D. A., J. H. Come, …, B. Caughey. 1994. Cell-free formation of protease-resistant prion protein. *Nature.* 370:471–474.
34. Adachi, M., M. So, …, Y. Goto. 2015. Supersaturation-limited and unlimited phase transitions compete to produce the pathway complexity in amyloid fibrillation. *J. Biol. Chem.* 290:18134–18145.
35. Bocharova, O. V., N. Makarava, …, I. V. Baskakov. 2006. Annealing prion protein amyloid fibrils at high temperature results in extension of a proteinase K-resistant core. *J. Biol. Chem.* 281:2373–2379.
36. Jones, E. M., and W. K. Surewicz. 2005. Fibril conformation as the basis of species- and strain-dependent seeding specificity of mammalian prion amyloids. *Cell.* 121:63–72.

37. Hill, A. F., S. Joiner, …, J. Collinge. 2003. Molecular classification of sporadic Creutzfeldt-Jakob disease. *Brain.* 126:1333–1346.

38. Zandomeneghi, G., M. R. Krebs, …, M. Fändrich. 2004. FTIR reveals structural differences between native β-sheet proteins and amyloid fibrils. *Protein Sci.* 13:3314–3321.

39. Lu, X., P. L. Wintrode, and W. K. Surewicz. 2007. Beta-sheet core of human prion protein amyloid fibrils as determined by hydrogen/deuterium exchange. *Proc. Natl. Acad. Sci. USA.* 104:1510–1515.

40. Tycko, R., R. Savtchenko, …, I. V. Baskakov. 2010. The α-helical C-terminal domain of full-length recombinant PrP converts to an in-register parallel β-sheet structure in PrP fibrils: evidence from solid state nuclear magnetic resonance. *Biochemistry.* 49:9488–9497.

41. Dutta, A., S. Chen, and W. K. Surewicz. 2013. The effect of β2-α2 loop mutation on amyloidogenic properties of the prion protein. *FEBS Lett.* 587:2918–2923.

42. Wedemeyer, W. J., E. Welker, …, H. A. Scheraga. 2000. Disulfide bonds and protein folding. *Biochemistry.* 39:4207–4216.

43. Baldwin, A. J., T. P. Knowles, …, C. M. Dobson. 2011. Metastability of native proteins and the phenomenon of amyloid formation. *J. Am. Chem. Soc.* 133:14160–14163.

44. Pace, C. N., G. R. Grimsley, …, B. J. Barnett. 1988. Conformational stability and activity of ribonuclease T1 with zero, one, and two intact disulfide bonds. *J. Biol. Chem.* 263:11820–11825.